

---

# Robust Bayesian Nonnegative Matrix Factorization with Implicit Regularizers

---

Jun Lu<sup>1</sup>Christine P. Chai<sup>2</sup>

## Abstract

We introduce a probabilistic model with implicit norm regularization for learning nonnegative matrix factorization (NMF) that is commonly used for predicting missing values and finding hidden patterns in the data, in which the matrix factors are latent variables associated with each data dimension. The nonnegativity constraint for the latent factors is handled by choosing priors with support on the nonnegative subspace, e.g., exponential density or distribution based on exponential function. Bayesian inference procedure based on Gibbs sampling is employed. We evaluate the model on several real-world datasets including Genomics of Drug Sensitivity in Cancer (GDSC  $IC_{50}$ ) and Gene body methylation with different sizes and dimensions, and show that the proposed Bayesian NMF  $GL_2^2$  and  $GL_{2,\infty}^2$  models lead to robust predictions for different data values and avoid overfitting compared with competitive Bayesian NMF approaches.

## 1. Introduction

Over the decades, low-rank matrix approximation methods provide a simple and effective approach to collaborative filtering for modeling user preferences (Marlin, 2003; Lim & Teh, 2007; Mnih & Salakhutdinov, 2007; Chen et al., 2009; Gillis, 2020; Lu & Ye, 2022). The idea behind such models is that preferences of a user are determined by a small number of unobserved factors (Salakhutdinov & Mnih, 2008). The Netflix competition winners, Koren et al. (2009), also employed nonnegative matrix factorization (NMF) in collaborative filtering to build a highly effective recommendation system. Nowadays nonnegative matrix factorization (NMF) models have remained popular, since the constraint

of nonnegativity makes the decompositional parts more interpretable (Wang et al., 2015; Song et al., 2019).

The goal of nonnegative matrix factorization (NMF) is to find a low rank representation of nonnegative data matrix as the product of two nonnegative matrices. Methods for factoring nonnegative matrices fall into two categories – non-probabilistic and probabilistic. Non-probabilistic methods typically use multiplicative updates for matrix factorization (Comon et al., 2009; Lu, 2022c). Probabilistic methods mean the factorization is done by maximum-a-posteriori (MAP) or Bayesian inference (Mnih & Salakhutdinov, 2007; Schmidt & Mohamed, 2009; Brouwer & Lio, 2017). Non-probabilistic solutions give a single point estimate that can easily lead to overfitting. For example, the two algorithms, one minimizing least squares error and the other minimizing the Kullback-Leibler divergence, proposed by Lee & Seung (1999; 2000) are not robust to sparse data (Brouwer & Lio, 2017; Lu & Ye, 2022). Therefore, probabilistic methods are favorable because they can quantify the model order and account for parameter uncertainties. The MAP estimates maximize the log-posterior over the parameters to train the model. However, the posterior distribution over the factors is intractable, so it is easy to fall into ad-hoc combinations of the parameters (Hofmann, 1999; Marlin, 2003; Salakhutdinov & Mnih, 2008). While we can apply various prior choices to reduce overfitting, Bayesian inference overcomes this issues by locating a full distribution over the nonnegative spaces.

In light of this, our attention is drawn to Bayesian approach for nonnegative matrix factorization. Given the matrix  $\mathbf{A}$ , the nonnegative factorization can be represented as  $\mathbf{A} = \mathbf{W}\mathbf{Z} + \mathbf{R} \in \mathbb{R}_+^{M \times N}$ , where the data matrix is approximately factorized into an  $M \times K$  nonnegative matrix  $\mathbf{W}$  and a  $K \times N$  nonnegative matrix  $\mathbf{Z}$ ; the residuals are captured by matrix  $\mathbf{R} \in \mathbb{R}^{M \times N}$  (having both positive and nonnegative entries). The first matrix  $\mathbf{W}$  contains low-rank column basis of the data matrix  $\mathbf{A}$  in columns, while  $\mathbf{Z}$  comprises row basis of  $\mathbf{A}$  in rows. It is also possible that the data matrix  $\mathbf{A}$  is sparse and incomplete, and the indices of observed entries can be represented by a mask matrix  $M \times N$  matrix  $\mathbf{O}$  that contains values of 0 and 1 to indicate the observation of each entry. The missing entries can be easily handled in Bayesian NMF inference by excluding the missing elements in the likelihood term. To be more concrete, in the Netflix

---

<sup>1</sup>Jun Lu, jun.lu.locky@gmail.com. <sup>2</sup>Christine P. Chai, cpchai21@gmail.com. Microsoft Corporation, Redmond WA 98052 USA. Disclaimer: The opinions and views expressed in this manuscript are those of the author and do not necessarily state or reflect those of Microsoft. Copyright 2022 by the author(s)/owner(s). August 22nd, 2022. Correspondence to: Jun Lu <jun.lu.locky@gmail.com>.

user preference context, the factorization means that the  $M \times N$  preference matrix of rating that  $M$  users assign to  $N$  movies is modeled by the product of an  $M \times K$  user feature matrix  $\mathbf{W}$  and a  $K \times N$  movie feature matrix  $\mathbf{Z}$  (Srebro & Jaakkola, 2003; Salakhutdinov & Mnih, 2008).

Project data vector  $\mathbf{a}_n$  ( $n$ -th column of  $\mathbf{A}$ ) to a smaller dimension  $\mathbf{z}_n \in \mathbb{R}^K$  with  $K < M$ , such that the *reconstruction error* measured by mean squared error (MSE) is minimized (assume  $K$  is known):

$$\min_{\mathbf{W}, \mathbf{Z}} \sum_{n=1}^N \sum_{m=1}^M (a_{mn} - \mathbf{w}_m^\top \mathbf{z}_n)^2 \cdot o_{mn}, \quad (1)$$

where  $\mathbf{W} = [\mathbf{w}_1^\top; \mathbf{w}_2^\top; \dots; \mathbf{w}_M^\top] \in \mathbb{R}_+^{M \times K}$  and  $\mathbf{Z} = [\mathbf{z}_1, \mathbf{z}_2, \dots, \mathbf{z}_N] \in \mathbb{R}_+^{K \times N}$  contain  $\mathbf{w}_m$ 's and  $\mathbf{z}_n$ 's as **rows and columns** respectively, and  $a_{mn}, o_{mn}$  are the  $(m, n)$ -th entries of data matrix  $\mathbf{A}$  and mask matrix  $\mathbf{O}$  respectively. The term in Eq. (1) is also known as the *Frobenius norm*. And it can be equivalently written as

$$\begin{aligned} L(\mathbf{W}, \mathbf{Z}) &= \sum_{n=1}^N \sum_{m=1}^M (a_{mn} - \mathbf{w}_m^\top \mathbf{z}_n)^2 \cdot o_{mn} \quad (2) \\ &= \|(\mathbf{WZ} - \mathbf{A}) \odot \mathbf{O}\|^2, \end{aligned}$$

where  $\odot$  represents the *Hadamard product (element-wise product)* between matrices.

We approach the nonnegative constraint by considering the NMF model as a latent factor model and we describe a fully specified graphical model for the problem and employ Bayesian learning methods to infer the latent factors. In this sense, explicit nonnegativity constraints are not required on the latent factors, since this is naturally taken care of by the appropriate choice of prior distribution, e.g., exponential density, half-normal density, truncated-normal density, or rectified-normal prior.

The main contribution of this paper is to propose a novel Bayesian NMF method which has implicit  $L_p$  norm regularization behind the model so that the models are more robust in various data types. We propose the Bayesian model called  $GL_2^2$  and  $GL_{2,\infty}^2$  NMF algorithms to both increase convergence performance and out-of-sample accuracy. While previous works propose somewhat algorithms that also have implicit regularization meaning (e.g., the  $GL_1^2$  model in Brouwer & Lio (2017)), an interpretation on the posterior parameters reveals that model is not robust especially when the entries of the observed matrix  $\mathbf{A}$  are large, in which case, the  $GL_1^2$  model tends to impose a regularization far too much and the end result lacks predictive ability. On the other hand, the proposed  $GL_2^2$  and  $GL_\infty$  models have simple conditional density forms. We show that our methods can be successfully applied to the sparse and imbalanced GDSC  $IC_{50}$  dataset; and also to the dense and balanced Gene body

methylation dataset. We also show that the proposed  $GL_2^2$  and  $GL_\infty$  models significantly increase the models' predictive accuracy (out-of-sample performance), compared with the standard Bayesian NMF models that has implicit interpretation of norm regularization.

## 2. Related Work

In this section, we review the Gaussian Exponential (GEE) model for computing nonnegative matrix factorization and its implicit regularization meaning behind the model.

### 2.1. Gaussian Exponential (GEE) Model

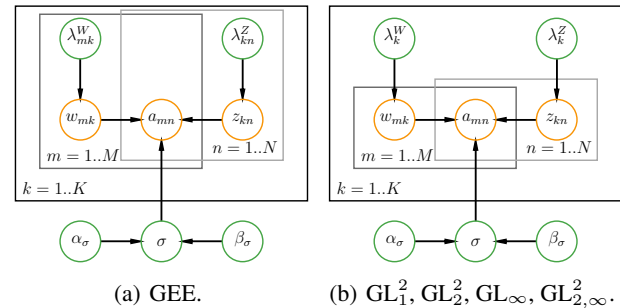


Figure 1: Graphical representation of  $GL_1^2$ ,  $GL_2^2$ ,  $GL_\infty$ , and  $GL_{2,\infty}^2$  models. Orange circles represent observed and latent variables, green circles denote prior variables, and plates represent repeated variables.  $\sigma^2$  denotes the variance parameter of normal distribution, and  $\alpha_\sigma, \beta_\sigma$  are the parameters of the prior over  $\sigma^2$ .

We view the data  $\mathbf{A}$  as being produced according to the probabilistic generative process shown in Figure 1(a). The observed  $(m, n)$ -th entry  $a_{mn}$  of matrix  $\mathbf{A}$  is modeled using a Gaussian likelihood function with variance  $\sigma^2$  and mean given by the latent decomposition  $\mathbf{w}_m^\top \mathbf{z}_n$  (Eq. (1)):

$$p(a_{mn} | \mathbf{w}_m^\top \mathbf{z}_n, \sigma^2) = \mathcal{N}(a_{mn} | \mathbf{w}_m^\top \mathbf{z}_n, \sigma^2), \quad (3)$$

where  $\mathcal{N}(a_{mn} | \mathbf{w}_m^\top \mathbf{z}_n, \sigma^2) = \sqrt{\frac{1}{2\pi\sigma^2}} \exp\{-\frac{1}{2\sigma^2}(a_{mn} - \mathbf{w}_m^\top \mathbf{z}_n)^2\}$  is a Gaussian distribution with mean  $\mu$  and variance  $\sigma^2$ .

We choose a conjugate prior over the data variance, an inverse-Gamma distribution with shape  $\alpha_\sigma$  and scale  $\beta_\sigma$ ,

$$p(\sigma^2 | \alpha_\sigma, \beta_\sigma) = \mathcal{G}^{-1}(\sigma^2 | \alpha_\sigma, \beta_\sigma), \quad (4)$$

where  $\mathcal{G}^{-1}(\sigma^2 | \alpha_\sigma, \beta_\sigma) = \frac{(\beta_\sigma)^{\alpha_\sigma}}{\Gamma(\alpha_\sigma)} (\sigma^2)^{-\alpha_\sigma-1} \cdot \exp\{-\frac{\beta_\sigma}{\sigma^2}\} \cdot u(\sigma^2)$  is an inverse-Gamma distribution,  $\Gamma(\cdot)$  is the gamma function, and  $u(\sigma^2)$  is the unit step function that has a value of 1 when  $\sigma^2 > 0$  and 0 otherwise.

While it can also be equivalently given a conjugate Gamma prior over the precision (inverse of variance) and we shall not repeat the details.

We treat the latent variables  $w_{mk}$ 's (and  $z_{kn}$ 's) as random variables. And we need prior densities over these latent variables to express beliefs for their values, e.g., nonnegativity in this context though there are many other constraints (semi-nonnegativity in Ding et al. (2008), interpolative prior in Lu (2022a;b), and discreteness in Gopalan et al. (2014; 2015)). Here we assume further that the latent variables  $w_{mk}$ 's are independently drawn from an exponential prior

$$w_{mk} \sim \mathcal{E}(w_{mk}|\lambda_{mk}^W), \quad (5)$$

where  $\mathcal{E}(w_{mk}|\lambda_{mk}^W) = \lambda_{mk}^W \exp\{-\lambda_{mk}^W \cdot w_{mk}\}u(w_{mk})$  is an exponential distribution.

Similarly, the latent variables  $z_{kn}$ 's are also drawn from the same exponential prior. This prior serves to enforce the nonnegativity constraint on the components  $\mathbf{W}$ ,  $\mathbf{Z}$ , and the conditional posterior density is a *truncated-normal distribution*. In some cases, the two sets of latent variables can be drawn from two different exponential priors (with different  $\lambda_{mk}^W$  and  $\lambda_{kn}^Z$  parameters for each component; see Figure 1(a)), e.g., enforcing sparsity in  $\mathbf{W}$  while non-sparsity in  $\mathbf{Z}$ . However, this is not the main interest of this paper and we shall not consider this scenario.

## 2.2. Priors as Regularization

Denote the prior parameters as  $\theta$  and follow the Bayes' rule, the posterior is proportional to product of likelihood and prior density:  $p(\theta|\mathbf{A}) \propto p(\mathbf{A}|\theta) \cdot p(\theta)$ , such that the log-likelihood follows

$$\begin{aligned} \log p(\theta|\mathbf{A}) &= \log p(\mathbf{A}|\theta) + \log p(\theta) + C_1 \\ &= \log \prod_{m,n=1}^{M,N} \mathcal{N}(a_{mn}|\mathbf{w}_m^\top \mathbf{z}_n, \sigma^2) + \log p(\mathbf{W}, \mathbf{Z}) + C_2 \\ &= -\frac{1}{2\sigma^2} (a_{mn} - \mathbf{w}_m^\top \mathbf{z}_n)^2 + \log p(\mathbf{W}, \mathbf{Z}) + C_3, \end{aligned}$$

where  $C_1, C_2, C_3$  are constants. The ultimate equation is the sum of the negative squared loss of the training fit and a regularization term over the factored components  $\mathbf{W}$ ,  $\mathbf{Z}$ . The prior distributions of  $\mathbf{W}$ ,  $\mathbf{Z}$  then act as a regularization that can prevent the model from overfitting the data and increase the predictive performance. To be more concrete, the regularizers on  $\mathbf{W}$  fall into four categories:

$$\begin{aligned} L_1 &= \sum_{m=1}^M \sum_{k=1}^K w_{mk}, & L_2^{1/2} &= \sum_{m=1}^M \sqrt{\sum_{k=1}^K w_{mk}}, \\ L_1^2 &= \sum_{m=1}^M \left( \sum_{k=1}^K w_{mk} \right)^2, & L_2^2 &= \sum_{m=1}^M \sum_{k=1}^K w_{mk}^2. \end{aligned} \quad (6)$$

We note that the  $L_2^2$  norm is equivalent to an independent Gaussian prior (GGG model in Brouwer & Lio (2017));

the  $L_1$  norm is equivalent to a Laplace prior (GLL model in Brouwer & Lio (2017)) in real-valued decomposition and is equivalent to an exponential prior (GEE model) in nonnegative matrix factorization.

## 2.3. Gaussian $L_1^2$ Prior ( $GL_1^2$ ) Model

The Gaussian  $L_1^2$  prior model follows immediately by replacing the  $L_1$  norm with  $L_1^2$  in the exponential prior:

$$p(\mathbf{W}|\lambda_k^W) \propto \exp\left\{-\frac{\lambda_k^W}{2} \sum_{m=1}^M \left(\sum_{k=1}^K w_{mk}\right)^2\right\}u(\mathbf{W}), \quad (7)$$

where  $u(\mathbf{W})$  denotes that all entries of  $\mathbf{W}$  are nonnegative. A similar prior is placed over component  $\mathbf{Z}$  (see Figure 1(b)).

## 3. Gaussian $L_p$ Prior Models

The proposed Gaussian  $L_p$  prior models highly rely on the implicit regularization in  $GL_1^2$  models. For any vector  $\mathbf{x} \in \mathbb{R}^n$ , the  $L_p$  norm is given by  $L_p(\mathbf{x}) = (\sum_{i=1}^n |x_i|^p)^{1/p}$  whose unit ball in 2-dimensional space is shown in Figure 2.

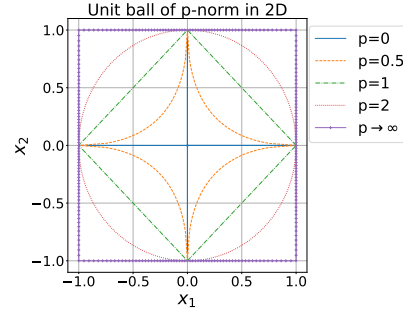


Figure 2: Unit ball of  $L_p$  norm in 2-dimensional space.

The  $L_1$  norm is known to have *sparse constraint*. We further extend the Bayesian models with  $L_2^2$  and  $L_\infty$  norms. We will show that the  $L_2^2$  and  $L_\infty$  norms in the Bayesian NMF context have this sparse constraint as well. To be more concrete, the prior for  $\mathbf{W}$  of  $GL_2^2$  model is given by

$$p(\mathbf{W}|\lambda_k^W) \propto \exp\left\{-\frac{\lambda_k^W}{2} \sum_{m=1}^M \left(\sum_{k=1}^K w_{mk}^2\right)\right\}u(\mathbf{W}). \quad (8)$$

And the prior for  $\mathbf{W}$  of  $GL_\infty$  model is given by

$$p(\mathbf{W}|\lambda_k^W) \propto \exp\left\{-\lambda_k^W \sum_{m=1}^M \max_k |w_{mk}|\right\}u(\mathbf{W}). \quad (9)$$

Note we remove the value of 2 in Eq. (9) for the denominator of  $\lambda_k^W$  for consistency issue which we will see shortly in the form of the conditional density in Table 1 or Eq. (21) in Appendix A.4.

	Conditional $w_{mk}$	$\widetilde{\mu}_{mk}$ (mean)	$\widetilde{\sigma}_{mk}^2$ (variance)
GEE	$\mathcal{TN}(w_{mk} \widetilde{\mu}_{mk}, \widetilde{\sigma}_{mk}^2)$	$\left(-\lambda_{mk}^W + \frac{1}{\sigma^2} \sum_{j=1}^N z_{kj} (a_{mj} - \sum_{i \neq k}^K w_{mi} z_{ij})\right) \widetilde{\sigma}_{mk}^2$	$\frac{\sigma^2}{\sum_{j=1}^N z_{kj}^2}$
GL $_1^2$	$\mathcal{TN}(w_{mk} \widetilde{\mu}_{mk}, \widetilde{\sigma}_{mk}^2)$	$\left(-\lambda_k^W \cdot \sum_{j \neq k}^K w_{mj} + \frac{1}{\sigma^2} \sum_{j=1}^N z_{kj} (a_{mj} - \sum_{i \neq k}^K w_{mi} z_{ij})\right) \widetilde{\sigma}_{mk}^2$	$\frac{\sigma^2}{\sum_{j=1}^N z_{kj}^2 + \sigma^2 \lambda_k^W}$
GL $_2^2$	$\mathcal{TN}(w_{mk} \widetilde{\mu}_{mk}, \widetilde{\sigma}_{mk}^2)$	$\left(\frac{1}{\sigma^2} \sum_{j=1}^N z_{kj} (a_{mj} - \sum_{i \neq k}^K w_{mi} z_{ij})\right) \widetilde{\sigma}_{mk}^2$	$\frac{\sigma^2}{\sum_{j=1}^N z_{kj}^2 + \sigma^2 \lambda_k^W}$
GL $_{\infty}$	$\mathcal{TN}(w_{mk} \widetilde{\mu}_{mk}, \widetilde{\sigma}_{mk}^2)$	$\left(-\lambda_k^W \cdot \mathbf{1}(w_{mk}) + \frac{1}{\sigma^2} \sum_{j=1}^N z_{kj} (a_{mj} - \sum_{i \neq k}^K w_{mi} z_{ij})\right) \widetilde{\sigma}_{mk}^2$	$\frac{\sigma^2}{\sum_{j=1}^N z_{kj}^2}$
GL $_{2,\infty}^2$	$\mathcal{TN}(w_{mk} \widetilde{\mu}_{mk}, \widetilde{\sigma}_{mk}^2)$	$\left(-\lambda_k^W \cdot \mathbf{1}(w_{mk}) + \frac{1}{\sigma^2} \sum_{j=1}^N z_{kj} (a_{mj} - \sum_{i \neq k}^K w_{mi} z_{ij})\right) \widetilde{\sigma}_{mk}^2$	$\frac{\sigma^2}{\sum_{j=1}^N z_{kj}^2 + \sigma^2 \lambda_k^W}$

Table 1: Posterior conditional densities of  $w_{mk}$ ’s for GEE, GL $_1^2$ , GL $_2^2$ , GL $_{\infty}$ , and GL $_{2,\infty}^2$  models. The difference is highlighted in red. The conditional densities of  $z_{kn}$ ’s are similar due to their symmetry to  $w_{mk}$ ’s.  $\mathcal{TN}(x|\mu, \tau^{-1}) = \frac{\sqrt{\frac{\tau}{2\pi}} \exp\{-\frac{\tau}{2}(x-\mu)^2\}}{1-\Phi(-\mu\sqrt{\tau})} u(x)$  is a truncated-normal (TN) density with zero density below  $x = 0$  and renormalized to integrate to one.  $\mu$  and  $\tau$  are known as the “parent” mean and “parent” precision.  $\Phi(\cdot)$  is the cumulative distribution function of standard normal density  $\mathcal{N}(0, 1)$ .

### 3.1. Gibbs Sampler

Here we use Gibbs sampling because it is easier and accurate to sample from the conditional distributions than the joint distribution (Hoff, 2009). Alternative methods are variational Bayesian inference or Metropolis-Hastings, but we shall not go into the details (Tichy et al., 2019). We shortly describe the posterior conditional density in this section, and the detailed derivation can be found in Appendix A. The conditional density of  $\sigma^2$  is an inverse-Gamma distribution by conjugacy,

$$p(\sigma^2|\mathbf{W}, \mathbf{Z}, \mathbf{A}) = \mathcal{G}^{-1}(\sigma^2|\widetilde{\alpha}_{\sigma}, \widetilde{\beta}_{\sigma}), \quad (10)$$

where  $\widetilde{\alpha}_{\sigma} = \frac{MN}{2} + \alpha_{\sigma}$ ,  $\widetilde{\beta}_{\sigma} = \frac{1}{2} \sum_{i,j=1}^{M,N} (a_{ij} - \mathbf{w}_i^{\top} \mathbf{z}_j)^2 + \beta_{\sigma}$ .

The conditional density of  $w_{mk}$ ’s for GEE, GL $_1^2$ , GL $_2^2$ , and GL $_{\infty}$  models are summarized in Table 1 where the difference is highlighted in red. A detailed derivation is provided in Appendix A. The posterior conditional density of  $z_{kn}$ ’s can be derived in a similar way. The full procedure is formulated in Algorithm 1.

**Sparse constraint in GEE** We note that there is a negative term  $-\lambda_{mk}^W$  in the posterior “parent” mean parameter  $\widetilde{\mu}_{mk}$  for GEE in Table 1 that can push the posterior “parent” mean  $\widetilde{\mu}_{mk}$  towards zero or negative values. The draws of  $\mathcal{TN}(w_{mk}|\widetilde{\mu}_{mk}, \widetilde{\sigma}_{mk}^2)$  will then be around zero thus imposing sparsity.

**Connection between GEE and GL $_1^2$  models** The second term  $\sigma^2 \lambda_k^W$  exists in the GL $_1^2$  denominator of the variance  $\widetilde{\sigma}_{mk}^2$ . When all else are held equal, the GL $_1^2$  has smaller variance than GEE, so the distribution of GL $_1^2$  is more clustered in a smaller range. This is actually a stronger constraint/regularizer than the GEE model.

Moreover, when  $\{\lambda_{mk}^W\}$  in GEE model and  $\{\lambda_k^W\}$  in GL $_1^2$  model are equal, the extra term  $\sum_{j \neq k}^K w_{mj}$  in GL $_1^2$  model

**Algorithm 1** Gibbs sampler for GEE, GL $_1^2$ , GL $_2^2$ , and GL $_{\infty}$  models (prior on the variance parameter  $\sigma^2$ ). The procedure presented here is for explanatory purposes, and vectorization can expedite the procedure. Users need to specify the total number of iterations  $T$ , the observed matrix  $\mathbf{A}$  of shape  $M \times N$ , and the latent dimension  $K$ . By default, uninformative priors are  $\{\lambda_{mk}^W\} = \{\lambda_{kn}^Z\} = 0.1$  (GEE);  $\{\lambda_{mk}^W\} = \{\lambda_k^Z\} = 0.1$  (GL $_1^2$ , GL $_2^2$ , GL $_{\infty}$ , GL $_{2,\infty}^2$ );  $\alpha_{\sigma} = \beta_{\sigma} = 1$  (inverse-Gamma prior in GEE, GL $_1^2$ , GL $_2^2$ , GL $_{\infty}$ , GL $_{2,\infty}^2$ );

- 1: **for**  $t = 1$  to  $T$  **do**
- 2:   **for**  $k = 1$  to  $K$  **do**
- 3:     **for**  $m = 1$  to  $M$  **do**
- 4:       Sample  $w_{mk}$  from  $p(w_{mk}|\cdot)$  from Table 1;
- 5:     **end for**
- 6:     **for**  $n = 1$  to  $N$  **do**
- 7:       Sample  $z_{kn}$  from  $p(z_{kn}|\cdot)$  (symmetry of  $w_{mk}$ );
- 8:     **end for**
- 9:   **end for**
- 10: Sample  $\sigma^2$  from  $p(\sigma^2|\mathbf{W}, \mathbf{Z}, \mathbf{A})$  (Eq. (10));
- 11: **end for**

plays an important role in controlling the sparsity of factored components in NMF context. To be more concrete, when the distribution of elements in matrix  $\mathbf{A}$  has a large portion of big values, the extra term  $\sum_{j \neq k}^K w_{mj}$  will be larger than 1 and thus enforce the posterior “parent” mean  $\widetilde{\mu}_{mk}$  of the truncated-normal density to be a small positive or even a negative value. This in turn constraints the draws of  $p(w_{mk}|\cdot)$  to be around zero thus favoring sparsity (see Section 4 for the experiment on GDSC  $IC_{50}$  dataset). On the contrary, when the entries in matrix  $\mathbf{A}$  are small, this extra term will be smaller than 1, the parameter  $\lambda_k^W$  has little impact on the posterior “parent” mean  $\widetilde{\mu}_{mk}$  which will possibly be a large value, and the factored component  $\mathbf{W}$  or  $\mathbf{Z}$  will be dense instead (also see Section 4 for the experiment on Gene body methylation dataset).

In this sense, the drawback of the GL $_1^2$  model is revealed

that it is not consistent and not robust for different types of the matrix  $\mathbf{A}$ . In contrast, the proposed  $GL_2^2$  and  $GL_{2,\infty}^2$  models are consistent and robust for different matrix types and impose a larger regularization compared with the GEE model such that its predictive performance is better (when the data matrix  $\mathbf{A}$  has large values).

**Connection between GEE,  $GL_2^2$ , and  $GL_{2,\infty}^2$  models** We observe that the posterior “parent” mean  $\widetilde{\mu}_{mk}$  in the  $GL_2^2$  model is larger than that in the GEE model since it does not contain the negative term  $-\lambda_{mk}^W$ . While the posterior “parent” variance is smaller than that in the GEE model, such that the conditional density of  $GL_2^2$  model is more clustered and it imposes a larger regularization in the sense of data/entry distribution. This can induce sparsity in the context of nonnegative matrix factorization. Moreover, the  $GL_2^2$  does not have the extra term  $\sum_{j \neq k}^K w_{mj}$  in  $GL_1^2$  model which causes the inconsistency for different types of matrix  $\mathbf{A}$  such that the proposed  $GL_2^2$  model is more robust.

**Connection between GEE and  $GL_\infty$  models** The posterior “parent” variance  $\widetilde{\sigma}_{mk}^2$  in the  $GL_2^2$  model is exactly the same as that in the GEE model. Denote  $\mathbb{1}(w_{mk})$  as the indicator whether  $w_{mk}$  is the largest one among  $k = 1, 2, \dots, K$ . Suppose further the condition  $\mathbb{1}(w_{mk})$  is satisfied, parameters  $\{\lambda_{mk}^W\}$  in GEE model and  $\{\lambda_k^W\}$  in  $GL_\infty$  model are equal, the “parent” mean  $\widetilde{\mu}_{mk}$  is the same as that in the GEE model as well. However, when  $w_{mk}$  is not the maximum value among  $\{w_{m1}, w_{m2}, \dots, w_{mK}\}$ , the “parent” mean  $\widetilde{\mu}_{mk}$  is larger than that in the GEE model since the  $GL_\infty$  model excludes this negative term. The  $GL_\infty$  model then has the interpretation that it has a *sparsity constraint* when  $w_{mk}$  is the maximum value; and it has a *relatively loose constraint* when  $w_{mk}$  is not the maximum value. Overall, the  $GL_\infty$  favors a loose regularization compared with the GEE model.

**Further extension:  $GL_{2,\infty}^2$  model** The  $GL_{2,\infty}^2$  model takes the advantages of both  $GL_2^2$  and  $GL_\infty$ , and the posterior parameters of  $GL_{2,\infty}^2$  are shown in Table 1. The implicit prior of the  $GL_{2,\infty}^2$  model can be obtained by

$$\begin{aligned} p(\mathbf{W} | \lambda_k^W) &\propto \\ \exp \left\{ \frac{-\lambda_k^W}{2} \sum_{m=1}^M \left( \sum_{k=1}^K w_{mk}^2 + 2 \max_k |w_{mk}| \right) \right\} u(\mathbf{W}). \end{aligned} \quad (11)$$

**Computational complexity** The adopted Gibbs sampling methods for GEE,  $GL_1^2$ ,  $GL_2^2$ ,  $GL_\infty$ , and  $GL_{2,\infty}^2$  models have complexity  $\mathcal{O}(MNK^2)$ , where the most expensive operation is the update on the conditional density of  $w_{mk}$ ’s and  $z_{kn}$ ’s.

## 4. Experiments

We conduct experiments with various analysis tasks to demonstrate the main advantages of the proposed  $GL_2^2$  and  $GL_{2,\infty}^2$  methods. We use two datasets from bioinformatics: The first one is the Genomics of Drug Sensitivity in Cancer dataset<sup>1</sup> (GDSC  $IC_{50}$ ) (Yang et al., 2012), which contains a wide range of drugs and their treatment outcomes on different cancer and tissue types (cell lines). Following Brouwer & Lio (2017), we preprocess the GDSC  $IC_{50}$  dataset by capping high values to 100, undoing the natural log transform, and casting them as integers. The second one is the Gene body methylation dataset (Koboldt et al., 2012), which gives the amount of methylation measured in the body region of 160 breast cancer driver genes. We multiply the values in Gene body methylation dataset by 20 and cast them as integers as well. A summary of the two datasets can be seen in Table 2 and their distributions are shown in Figure 5. The GDSC  $IC_{50}$  dataset has a larger range whose values are unbalanced (either small as 0 or larger as 100); while the Gene body methylation dataset has a smaller range whose values seem balanced. We can see that the GDSC  $IC_{50}$  is relatively a large dataset whose matrix rank is 139 and the Gene body methylation data tends to be small whose matrix rank is 160.

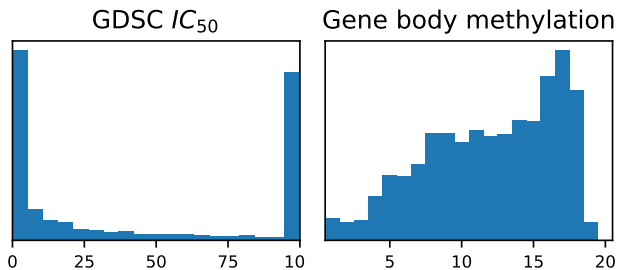


Figure 5: Data distribution of GDSC  $IC_{50}$  and Gene body methylation datasets.

Dataset	Rows	Columns	Fraction obs.
GDSC $IC_{50}$	707	139	0.806
Gene body meth.	160	254	1.000

Table 2: Dataset description. Gene body methylation is relatively a small dataset and the GDSC  $IC_{50}$  tends to be large. The description provides the number of rows, columns, and the fraction of entries that are observed.

The same parameter initialization is adopted in each scenario. We compare the results in terms of convergence speed and generalization. In a wide range of scenarios across various models,  $GL_2^2$  and  $GL_{2,\infty}^2$  improve convergence rates, and lead to out-of-sample performance that is as good or better than existing Bayesian NMF models.

<sup>1</sup><https://www.cancerrxgene.org/>

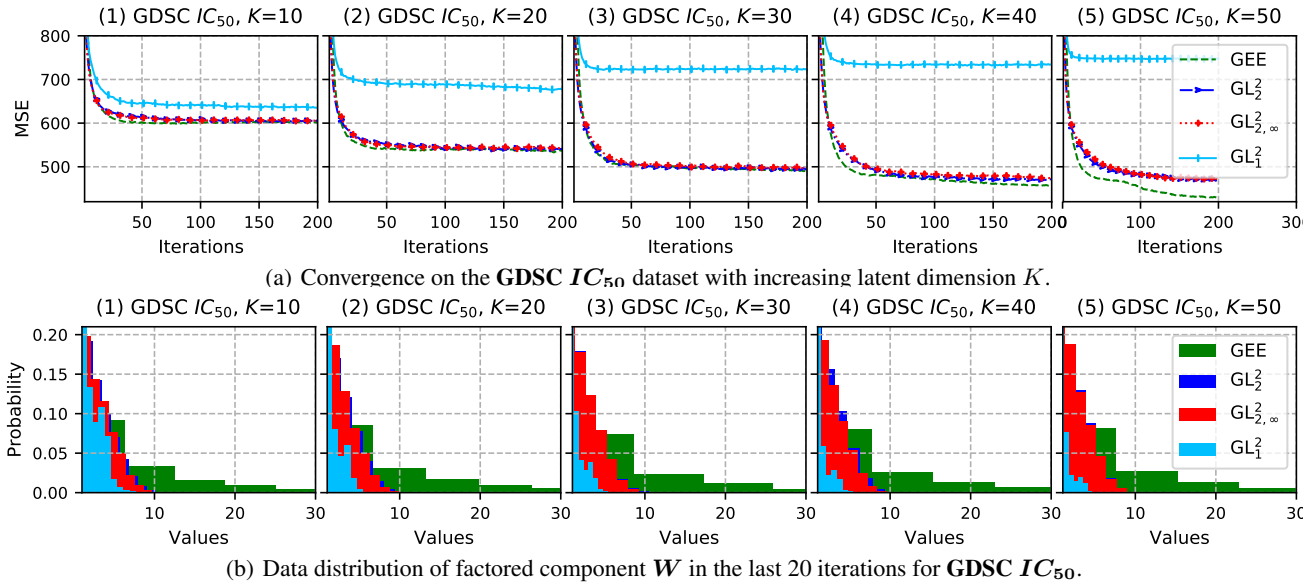


Figure 3: Convergence of the models on the GDSC  $IC_{50}$  (upper) and the distribution of factored  $\mathbf{W}$  (lower), measuring the training data fit (mean squared error). When we increase latent dimension  $K$ , the GEE and the proposed  $GL_2^2$  and  $GL_{2,\infty}^2$  algorithms continue to increase the performance; while  $GL_1^2$  start to decrease.

#### 4.1. Hyperparameters

We follow the default hyperparameter setups in Brouwer & Lio (2017). We use  $\{\lambda_{mk}^W\} = \{\lambda_{kn}^Z\} = 0.1$  (GEE);  $\{\lambda_k^W\} = \{\lambda_k^Z\} = 0.1$  ( $GL_1^2$ ,  $GL_2^2$ ,  $GL_{2,\infty}^2$ ); uninformative  $\alpha_\sigma = \beta_\sigma = 1$  (inverse-Gamma prior in GEE,  $GL_1^2$ ,  $GL_2^2$ ,  $GL_{2,\infty}^2$ ). These are very weak prior choices and the models are insensitive to them (Brouwer & Lio, 2017). As long as the hyperparameters are set, the observed or unobserved variables are initialized from random draws as this initialization procedure provides a better initial guess of the right patterns in the matrices. In all experiments, we run the Gibbs sampler 500 iterations with a burn-in of 300 iterations as the convergence analysis shows the algorithm can converge in fewer than 200 iterations.

#### 4.2. Convergence Analysis

**GDSC  $IC_{50}$  with relatively large entries** Firstly we compare the convergence in terms of iterations on the GDSC  $IC_{50}$  and Gene body methylation datasets. We run each model with  $K = \{10, 20, 30, 40, 50\}$ , and the loss is measured by mean squared error (MSE). Figure 3(a) shows the average convergence results of ten repeats and Figure 3(b) shows the distribution of entries of the factored  $\mathbf{W}$  for the last 20 iterations on the GDSC  $IC_{50}$  dataset. The result is consistent with our analysis (Section 3.1, the connection between different models). Since the values of the data matrix for GDSC  $IC_{50}$  dataset is large, the posterior ‘‘parent’’ mean  $\widetilde{\mu}_{mk}$  in  $GL_1^2$  model is approaching zero or even negative, thus it has a larger regularization than GEE model. This makes the  $GL_1^2$  model converge to a worse performance.

$GL_2^2$  and  $GL_{2,\infty}^2$  models, on the contrary, impose looser regularization than the  $GL_1^2$  model, and the convergence performances are close to that of the GEE model.

#### Gene body methylation with relatively small entries

Figure 4(a) further shows the average convergence results of ten repeats, and Figure 4(b) shows the distribution of the entries of the factored  $\mathbf{W}$  for the last 20 iterations on the Gene body methylation dataset. The situation is different for the  $GL_1^2$  model since the range of the entries of the Gene body methylation dataset is smaller than that of the GDSC  $IC_{50}$  dataset (see Figure 5). This makes the  $-\lambda_k^W \cdot \sum_{j \neq k}^K w_{mj}$  term of posterior ‘‘parent’’ mean  $\widetilde{\mu}_{mk}$  in  $GL_1^2$  model approach zero (see Table 1), and the model then favors a looser regularization than the GEE model.

The situation can be further presented by the distribution of the factored component  $\mathbf{W}$  on the GDSC  $IC_{50}$  (Figure 3(b)) and on the Gene body methylation (Figure 4(b)). GEE model has larger values of  $\mathbf{W}$  on the former dataset and smaller values on the latter; while  $GL_1^2$  has smaller values of  $\mathbf{W}$  on the former dataset and larger values on the latter. In other words, the regularization of the GEE and  $GL_1^2$  is inconsistent on the two different data matrices. In comparison, the proposed  $GL_2^2$  and  $GL_{2,\infty}^2$  are consistent on different datasets, making them more robust algorithms to compute NMF.

Table 3 shows the mean values of the factored component  $\mathbf{W}$  in the last 20 iterations for GDSC  $IC_{50}$  (upper table) and Gene body methylation (lower table) where the value in the parentheses is the sparsity evaluated by taking the percentage of values smaller than 0.1. The inconsistency of

## Robust Bayesian Nonnegative Matrix Factorization with Implicit Regularizers

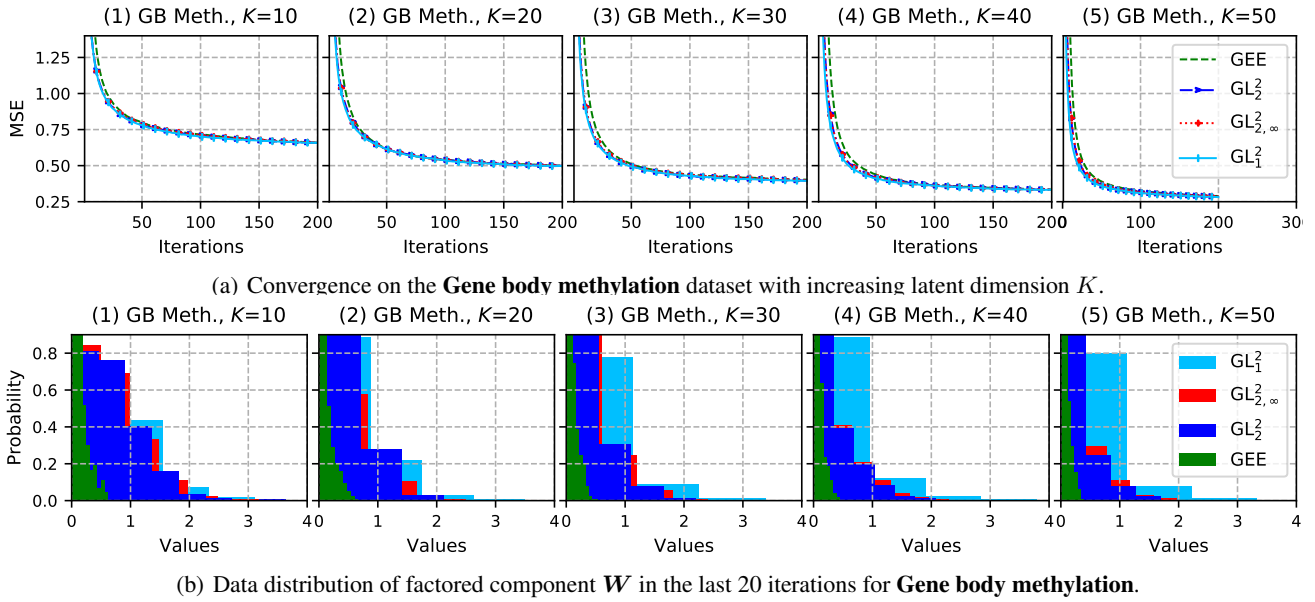


Figure 4: Convergence of the models on the Gene body methylation dataset (upper) and the distribution of factored  $\mathbf{W}$  (lower), measuring the training data fit (mean squared error). When we increase latent dimension  $K$ , all the models continue to increase the performance.

$K$	GEE	$GL_1^2$	$GL_2^2$	$GL_{2,\infty}^2$
10	8.1 (1.9)	1.3 (10.3)	2.4 (3.8)	2.4 (4.5)
20	8.6 (1.5)	0.8 (14.7)	2.3 (4.1)	2.2 (4.4)
30	8.7 (1.4)	0.7 (17.3)	2.2 (4.3)	2.2 (4.4)
40	8.3 (1.5)	0.6 (19.4)	2.2 (4.4)	2.2 (4.4)
50	8.0 (1.6)	0.5 (21.2)	2.2 (4.1)	2.2 (4.2)
10	0.1 (80.4)	0.7 (11.4)	0.7 (11.5)	0.7 (12.7)
20	0.1 (87.8)	0.6 (16.2)	0.5 (21.3)	0.5 (21.0)
30	0.0 (90.2)	0.6 (18.2)	0.3 (37.1)	0.3 (36.4)
40	0.0 (92.2)	0.6 (20.8)	0.3 (48.9)	0.3 (49.1)
50	0.0 (93.0)	0.5 (22.8)	0.2 (58.4)	0.2 (58.4)

Table 3: Mean values of the factored component  $\mathbf{W}$  in the last 20 iterations, where the value in the parentheses is the sparsity evaluated by taking the percentage of values smaller than 0.1, for GDSC  $IC_{50}$  (upper table) and Gene body methylation (lower table). The inconsistency of GEE and  $GL_1^2$  for different matrices can be observed.

GEE and  $GL_1^2$  for different matrices can be observed (either large sparsity or small sparsity), while the results for the proposed  $GL_2^2$  and  $GL_{2,\infty}^2$  models are more consistent.

### 4.3. Predictive Analysis

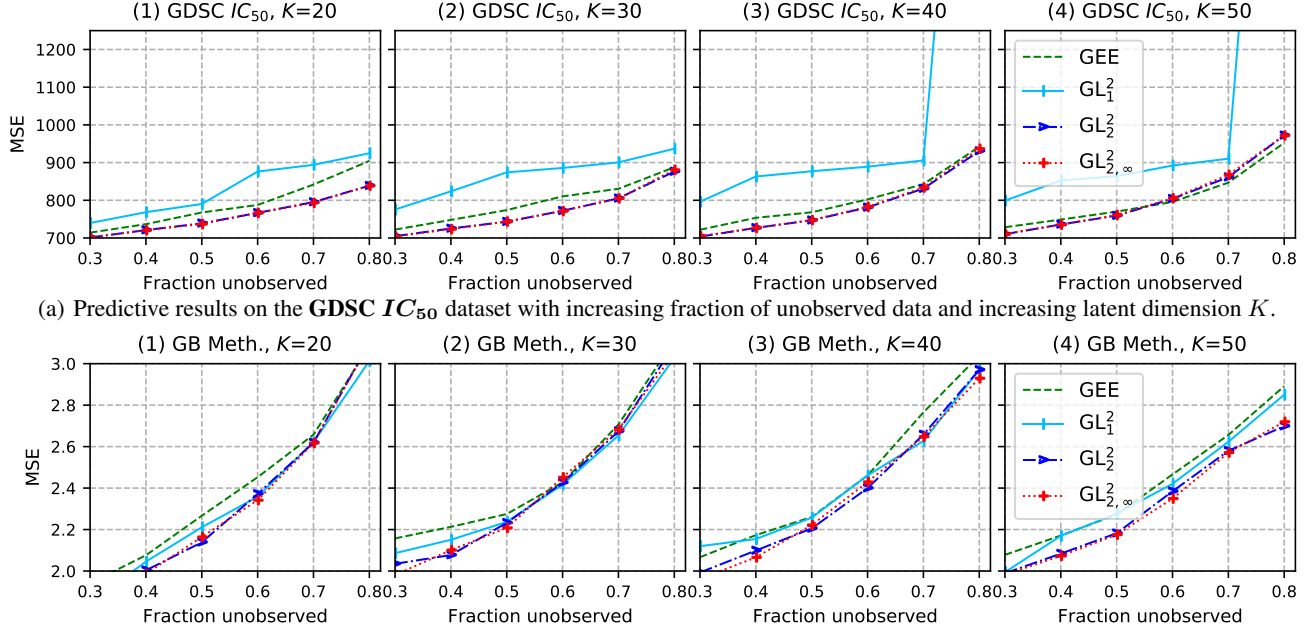
The training performances of the GEE,  $GL_2^2$ , and  $GL_{2,\infty}^2$  models steadily improve as the model complexity grows. Inspired by this result, we measure the predictive performance when the sparsity of the data increases to see whether the models overfit or not. For different fractions of unobserved data, we randomly split the data based on that fraction, train the model on the observed data, and measure the performance on the held-out test data. Again, we increase  $K$  from

Unobs.	$K$	GEE	$GL_1^2$	$GL_2^2$	$GL_{2,\infty}^2$
60%	20	787.60	880.36	<b>769.24</b>	<b>768.27</b>
	30	810.39	888.47	<b>774.53</b>	<b>773.27</b>
	40	802.39	892.01	<b>783.26</b>	<b>784.30</b>
	50	<b>795.72</b>	895.05	<b>806.14</b>	<b>807.44</b>
	20	841.74	895.77	<b>798.44</b>	<b>796.15</b>
70%	30	830.45	902.48	<b>807.37</b>	<b>806.61</b>
	40	<b>842.70</b>	907.65	<b>832.67</b>	<b>835.89</b>
	50	<b>846.83</b>	1018.97 $\uparrow$	<b>864.58</b>	<b>869.15</b>
	20	904.39	926.72	<b>842.24</b>	<b>841.84</b>
80%	30	<b>887.63</b>	938.92	<b>879.30</b>	<b>883.57</b>
	40	<b>942.44</b>	2634.69	<b>935.09</b>	<b>939.77</b>
	50	<b>952.45</b>	2730.30 $\uparrow$	<b>974.01</b>	<b>973.75</b>

Table 4: Mean squared error measure when the percentage of unobserved data is 60% (upper table), 70% (middle table), or 80% (lower table) for the GDSC  $IC_{50}$  dataset. The performance of the proposed  $GL_2^2$  and  $GL_{2,\infty}^2$  models is only slightly worse when we increase the fraction of unobserved from 60% to 80%; while the performance of  $GL_1^2$  becomes extremely poor. Similar observations occur in the Gene body methylation experiment. The symbol  $\uparrow$  means the performance becomes extremely worse.

$K = 20$  to  $K = 30, 40, 50$  for all models. The average MSE of ten repeats is given in Figure 6. We still observe the inconsistency issue in the  $GL_1^2$  model, the predictive performance of it is as good as that of the proposed  $GL_2^2$  and  $GL_{2,\infty}^2$  models on the Gene body methylation dataset; while the predictive results of the  $GL_1^2$  model are extremely poor on the GDSC  $IC_{50}$  dataset.

For the GDSC  $IC_{50}$  dataset, the proposed  $GL_2^2$  and  $GL_{2,\infty}^2$  models perform best when the latent dimensions are  $K =$



(a) Predictive results on the **GDSC  $IC_{50}$**  dataset with increasing fraction of unobserved data and increasing latent dimension  $K$ .  
 (b) Predictive results on **Gene body methylation** dataset with increasing fraction of unobserved data and increasing latent dimension  $K$ .  
 Figure 6: Predictive results on the **GDSC  $IC_{50}$**  (upper) and **Gene body methylation** (lower) datasets. We measure the predictive performance (mean squared error) on a held-out dataset for different fractions of unobserved data.

20, 30, 40; when  $K = 50$  and the fraction of unobserved data increases, the GEE model is slightly better. As aforementioned, the  $GL_1^2$  performs the worst on this dataset; and when the fraction of unobserved data increases or  $K$  increases, the predictive results of  $GL_1^2$  deteriorate quickly.

For the Gene body methylation dataset, the predictive performance of  $GL_1^2$ ,  $GL_2^2$  and  $GL_{2,\infty}^2$  models are close ( $GL_1^2$  has a slightly larger error). The GEE model performs the worst on this dataset.

The comparison on the two sets shows the proposed  $GL_2^2$  and  $GL_{2,\infty}^2$  models have both better in-sample and out-of-sample performance, making them a more robust choice in predicting missing entries.

Table 4 shows MSE predictions of different models when the fractions of unobserved data is 60%, 70%, and 80% respectively. We observe that the performances of the proposed  $GL_2^2$  and  $GL_{2,\infty}^2$  models are only slightly worse when we increase the fraction of unobserved from 60% to 80%. This indicates the proposed  $GL_2^2$  and  $GL_{2,\infty}^2$  models are more robust with less overfitting. While for the  $GL_1^2$  model, the performance becomes extremely poor in this scenario.

#### 4.4. Noise Sensitivity

Finally, we measure the noise sensitivity of different models with predictive performance when the datasets are noisy. To see this, we add different levels of Gaussian noise to the data. We add levels of  $\{0\%, 10\%, 20\%, 50\%, 100\%\}$  noise-to-signal ratio noise (which is the ratio of the vari-

ance of the added Gaussian noise to the variance of the data). The results for the GDSC  $IC_{50}$  with  $K = 10$  are shown in Figure 7. The results are the average performance over 10 repeats. We observe that the proposed  $GL_2^2$  and  $GL_{2,\infty}^2$  models perform slightly better than other NMF models. The proposed  $GL_2^2$  and  $GL_{2,\infty}^2$  models perform notably better when the noise-to-signal ratio is smaller than 10% and slightly better when the ratio is larger than 20%. Similar results can be found on the Gene body methylation dataset and other  $K$  values and we shall not repeat the details.

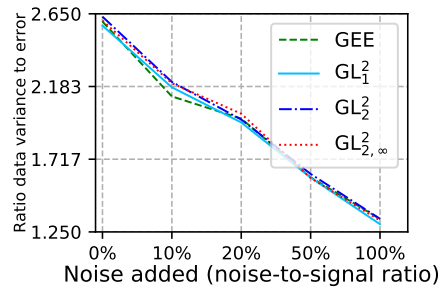


Figure 7: Ratio of the variance of data to the MSE of the predictions, the higher the better.

## 5. Conclusion

This article proposes a general framework of Bayesian NMF with implicit norm regularization. This is a simple and computationally efficient algorithm that requires no extra computation and is easy to implement for nonnegative matrix factorization. Overall, we show that the proposed  $GL_2^2$



and  $GL_{2,\infty}^2$  models are versatile algorithms that have better convergence results and out-of-sample performance on datasets with both small and large range of values.  $GL_{2,\infty}^2$  and  $GL_{2,\infty}^2$  are able to avoid problems of overfitting, which are common in the standard non-probabilistic NMF model (Schmidt & Mohamed, 2009) and other Bayesian NMF models (Brouwer & Lio, 2017).

## References

- Brouwer, Thomas and Lio, Pietro. Prior and likelihood choices for Bayesian matrix factorisation on small datasets. *arXiv preprint arXiv:1712.00288*, 2017.
- Chen, Gang, Wang, Fei, and Zhang, Changshui. Collaborative filtering using orthogonal nonnegative matrix tri-factorization. *Information Processing & Management*, 45(3):368–379, 2009.
- Comon, Pierre, Luciani, Xavier, and De Almeida, André LF. Tensor decompositions, alternating least squares and other tales. *Journal of Chemometrics: A Journal of the Chemometrics Society*, 23(7-8):393–405, 2009.
- Ding, Chris HQ, Li, Tao, and Jordan, Michael I. Convex and semi-nonnegative matrix factorizations. *IEEE Transactions on Pattern Analysis and Machine Intelligence*, 32(1):45–55, 2008.
- Gillis, Nicolas. *Nonnegative Matrix Factorization*. SIAM (Society for Industrial and Applied Mathematics), 2020.
- Gopalan, Prem, Ruiz, Francisco J, Ranganath, Rajesh, and Blei, David. Bayesian nonparametric Poisson factorization for recommendation systems. In *Artificial Intelligence and Statistics*, pp. 275–283. PMLR (Proceedings of Machine Learning Research), 2014.
- Gopalan, Prem, Hofman, Jake M, and Blei, David M. Scalable recommendation with hierarchical Poisson factorization. In *Proceedings of the Thirty-First Conference on Uncertainty in Artificial Intelligence (UAI)*, pp. 326–335, 2015.
- Hoff, Peter D. *A First Course in Bayesian Statistical Methods*. Springer, New York NY, United States, 2009.
- Hofmann, Thomas. Probabilistic latent semantic analysis. In *Proceedings of the Fifteenth Conference on Uncertainty in Artificial Intelligence (UAI)*, pp. 289–296, 1999.
- Koboldt, Daniel C, Fulton, Robert S, McLellan, Michael D, Schmidt, Heather, Kalicki-Veizer, Joelle, McMichael, Joshua F, Fulton, Lucinda L, Dooling, David J, Ding, Li, Mardis, Elaine R, et al. Comprehensive molecular portraits of human breast tumours. *Nature*, 490(7418):61–70, 2012.
- Koren, Yehuda, Bell, Robert, and Volinsky, Chris. Matrix factorization techniques for recommender systems. *Computer*, 42(8): 30–37, 2009.
- Lee, Daniel and Seung, H Sebastian. Algorithms for non-negative matrix factorization. *Advances in Neural Information Processing Systems*, 13, 2000.
- Lee, Daniel D and Seung, H Sebastian. Learning the parts of objects by non-negative matrix factorization. *Nature*, 401(6755): 788–791, 1999.
- Lim, Yew Jin and Teh, Yee Whye. Variational Bayesian approach to movie rating prediction. In *Proceedings of KDD Cup and Workshop*, volume 7, pp. 15–21. Citeseer, 2007.
- Lu, Jun. Bayesian low-rank interpolative decomposition for complex datasets. *arXiv preprint arXiv:2205.14825, Studies in Engineering and Technology*, 9(1):1–12, 2022a.
- Lu, Jun. Comparative study of inference methods for interpolative decomposition. *arXiv preprint arXiv:2206.14542*, 2022b.
- Lu, Jun. Matrix decomposition and applications. *arXiv preprint arXiv:2201.00145*, 2022c.
- Lu, Jun and Ye, Xuanyu. Flexible and hierarchical prior for Bayesian nonnegative matrix factorization. *arXiv preprint arXiv:2205.11025*, 2022.
- Marlin, Benjamin M. Modeling user rating profiles for collaborative filtering. *Advances in Neural Information Processing Systems*, 16, 2003.
- Mnih, Andriy and Salakhutdinov, Russ R. Probabilistic matrix factorization. *Advances in Neural Information Processing Systems*, 20, 2007.
- Salakhutdinov, Ruslan and Mnih, Andriy. Bayesian probabilistic matrix factorization using Markov chain Monte Carlo. In *Proceedings of the 25th International Conference on Machine Learning*, pp. 880–887, 2008.
- Schmidt, Mikkel N and Mohamed, Shakir. Probabilistic non-negative tensor factorization using Markov chain Monte Carlo. In *2009 17th European Signal Processing Conference*, pp. 1918–1922. IEEE, 2009.
- Schmidt, Mikkel N, Winther, Ole, and Hansen, Lars Kai. Bayesian non-negative matrix factorization. In *International Conference on Independent Component Analysis and Signal Separation*, pp. 540–547. Springer, 2009.
- Song, Yan, Li, Ming, Luo, Xin, Yang, Guisong, and Wang, Chongjing. Improved symmetric and nonnegative matrix factorization models for undirected, sparse and large-scaled networks: A triple factorization-based approach. *IEEE Transactions on Industrial Informatics*, 16(5):3006–3017, 2019.
- Srebro, Nathan and Jaakkola, Tommi. Weighted low-rank approximations. In *Proceedings of the 20th International Conference on Machine Learning (ICML-03)*, pp. 720–727, 2003.
- Tichý, Ondřej, Bódiová, Lenka, and Šmídl, Václav. Bayesian non-negative matrix factorization with adaptive sparsity and smoothness prior. *IEEE Signal Processing Letters*, 26(3):510–514, 2019.
- Wang, Mengmeng, Zuo, Wanli, and Wang, Ying. A multidimensional nonnegative matrix factorization model for retweeting behavior prediction. *Mathematical Problems in Engineering*, 2015, 2015.
- Yang, Wanjuan, Soares, Jorge, Greninger, Patricia, Edelman, Elena J, Lightfoot, Howard, Forbes, Simon, Bindal, Nidhi, Beare, Dave, Smith, James A, Thompson, I Richard, et al. Genomics of drug sensitivity in cancer (GDSC): A resource for therapeutic biomarker discovery in cancer cells. *Nucleic Acids Research*, 41(D1):D955–D961, 2012.

## A. Gibbs Sampling Algorithms of NMF Models

We give the posteriors for several Bayesian NMF models that we compare in the paper, namely, the GEE,  $GL_1^2$ ,  $GL_2^2$ , and  $GL_\infty$  models. The derivation for  $GL_{2,\infty}^2$  model is just the same as the  $GL_2^2$  and  $GL_\infty$  models. For clarity, the parameters for posterior densities are denoted using symbols with a widetilde, e.g.,  $\widetilde{\mu}$  and  $\widetilde{\sigma}^2$  for the posterior mean and variance respectively.

### A.1. Gaussian Likelihood with Exponential Priors (GEE) Model

The Gaussian Exponential-Exponential (GEE) model is perhaps the simplest one for Bayesian NMF (Schmidt et al., 2009) where each entry  $a_{mn}$  of matrix  $\mathbf{A}$  is again modeled using a Gaussian likelihood with variance  $\sigma^2$  and mean given by the latent decomposition  $\mathbf{w}_m^\top \mathbf{z}_n$  (Eq. (3), this will be default for  $GL_1^2$ ,  $GL_2^2$ ,  $GL_\infty$ , and  $GL_{2,\infty}^2$  models as well). The graphical representation is shown in Figure 8(a):

The model places independent exponential priors over the entries of  $\mathbf{W}$ ,  $\mathbf{Z}$ ,

$$\begin{aligned} w_{mk} &\sim \mathcal{E}(w_{mk} | \lambda_{mk}^W), & z_{kn} &\sim \mathcal{E}(z_{kn} | \lambda_{kn}^Z); \\ p(\mathbf{W} | \{\lambda_{mk}^W\}) &= \prod_{m,k=1}^{M,K} \mathcal{E}(w_{mk} | \lambda_{mk}^W), & p(\mathbf{Z} | \{\lambda_{kn}^Z\}) &= \prod_{k,n=1}^{K,N} \mathcal{E}(z_{kn} | \lambda_{kn}^Z). \end{aligned}$$

Denote  $\boldsymbol{\lambda}^W$  as the  $M \times K$  matrix containing all  $\{\lambda_{mk}^W\}$  entries,  $\boldsymbol{\lambda}^Z$  as the  $K \times N$  matrix including all  $\{\lambda_{kn}^Z\}$  values, and  $\mathbf{W}_{-mk}$  as all elements of  $\mathbf{W}$  except  $w_{mk}$ . The product of a Gaussian and an exponential distribution leads to a truncated-normal posterior,

$$\begin{aligned} &p(w_{mk} | \sigma^2, \mathbf{W}_{-mk}, \mathbf{Z}, \boldsymbol{\lambda}^W, \boldsymbol{\lambda}^Z, \mathbf{A}) = p(w_{mk} | \sigma^2, \mathbf{W}_{-mk}, \mathbf{Z}, \lambda_{mk}^W, \mathbf{A}) \\ &\propto p(\mathbf{A} | \mathbf{W}, \mathbf{Z}, \sigma^2) \times p(w_{mk} | \lambda_{mk}^W) = \prod_{i,j=1}^{M,N} \mathcal{N}(a_{ij} | \mathbf{w}_i^\top \mathbf{z}_j, \sigma^2) \times \mathcal{E}(w_{mk} | \lambda_{mk}^W) \\ &\propto \exp \left\{ -\frac{1}{2\sigma^2} \sum_{i,j=1}^{M,N} (a_{ij} - \mathbf{w}_i^\top \mathbf{z}_j)^2 \right\} \times \cancel{\lambda_{mk}^W} \exp(-\lambda_{mk}^W \cdot w_{mk}) u(w_{mk}) \\ &\propto \exp \left\{ -\frac{1}{2\sigma^2} \sum_{j=1}^N (a_{mj} - \mathbf{w}_m^\top \mathbf{z}_j)^2 \right\} \cdot \exp(-\lambda_{mk}^W \cdot w_{mk}) u(w_{mk}) \\ &\propto \exp \left\{ -\frac{1}{2\sigma^2} \sum_{j=1}^N \left( w_{mk}^2 z_{kj}^2 + 2w_{mk} z_{kj} \left( \sum_{i \neq k}^K w_{mi} z_{ij} - a_{mj} \right) \right) \right\} \cdot \exp(-\lambda_{mk}^W \cdot w_{mk}) u(w_{mk}) \\ &\propto \exp \left\{ -\underbrace{\left( \frac{\sum_{j=1}^N z_{kj}^2}{2\sigma^2} \right)}_{1/(2\widetilde{\sigma}_{mk}^2)} w_{mk}^2 + w_{mk} \underbrace{\left( -\lambda_{mk}^W + \frac{1}{\sigma^2} \sum_{j=1}^N z_{kj} \left( a_{mj} - \sum_{i \neq k}^K w_{mi} z_{ij} \right) \right)}_{\widetilde{\sigma}_{mk}^2 \cdot \widetilde{\mu}_{mk}} \right\} \cdot u(w_{mk}) \\ &\propto \mathcal{N}(w_{mk} | \widetilde{\mu}_{mk}, \widetilde{\sigma}_{mk}^2) \cdot u(w_{mk}) = \mathcal{TN}(w_{mk} | \widetilde{\mu}_{mk}, \widetilde{\sigma}_{mk}^2), \end{aligned} \tag{12}$$

where

$$\widetilde{\sigma}_{mk}^2 = \frac{\sigma^2}{\sum_{j=1}^N z_{kj}^2} \tag{13}$$

is the posterior variance of the normal distribution with mean  $\widetilde{\mu}_{mk}$ ,

$$\widetilde{\mu}_{mk} = \left( -\lambda_{mk}^W + \frac{1}{\sigma^2} \sum_{j=1}^N z_{kj} \left( a_{mj} - \sum_{i \neq k}^K w_{mi} z_{ij} \right) \right) \cdot \widetilde{\sigma}_{mk}^2 \tag{14}$$

is the posterior mean of the normal distribution and  $\mathcal{TN}(x|\mu, \sigma^2)$  is the *truncated normal density* with “parent” mean  $\mu$  and “parent” variance  $\sigma^2$ .

Or after rearrangement, the posterior density of  $w_{mk}$  can be equivalently described by

$$p(w_{mk}|\sigma^2, \mathbf{W}_{-mk}, \mathbf{Z}, \lambda, \mathbf{A}) = \mathcal{RN}(w_{mk}|\widehat{\mu}_{mk}, \widehat{\sigma}_{mk}^2, \lambda_{mk}^W),$$

where  $\widehat{\sigma}_{mk}^2 = \widetilde{\sigma}_{mk}^2 = \frac{\sigma^2}{\sum_{j=1}^N z_{kj}^2}$  is the posterior “parent” variance of the normal distribution with “parent” mean  $\widehat{\mu}_{mk}$ ,

$$\widehat{\mu}_{mk} = \frac{1}{\sum_{j=1}^N z_{kj}^2} \cdot \sum_{j=1}^N z_{kj} \left( a_{mj} - \sum_{i \neq k}^K w_{mi} z_{ij} \right).$$

Due to symmetry, a similar expression for  $z_{kn}$  can be easily derived.

The conditional density of  $\sigma^2$  depends on its parents ( $\alpha_\sigma, \beta_\sigma$ ), children ( $\mathbf{A}$ ), and co-parents ( $\mathbf{W}, \mathbf{Z}$ ) in the graph. And it is an inverse-gamma distribution (by conjugacy),

$$p(\sigma^2|\mathbf{W}, \mathbf{Z}, \mathcal{X}^W, \mathcal{X}^Z, \mathbf{A}) = p(\sigma^2|\mathbf{W}, \mathbf{Z}, \mathbf{A}) = \mathcal{G}^{-1}(\sigma^2|\widetilde{\alpha}_\sigma, \widetilde{\beta}_\sigma),$$

$$\widetilde{\alpha}_\sigma = \frac{MN}{2} + \alpha_\sigma, \quad \widetilde{\beta}_\sigma = \frac{1}{2} \sum_{m,n=1}^{M,N} (\mathbf{A} - \mathbf{W}\mathbf{Z})_{mn}^2 + \beta_\sigma. \quad (15)$$

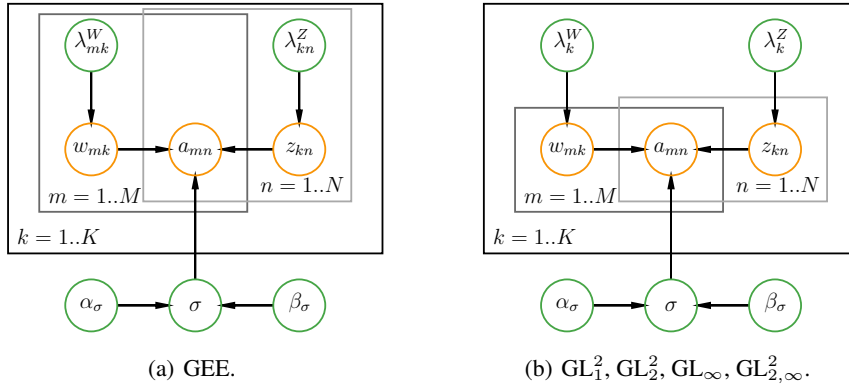


Figure 8: Same as Figure 1 with higher resolution. Graphical model representation of GEE,  $GL_1^2$ ,  $GL_2^2$ ,  $GL_\infty$ , and  $GL_{2,\infty}^2$  models. Orange circles represent observed and latent variables, green circles denote prior variables, and plates represent repeated variables.

## A.2. Gaussian Likelihood with $L_1^2$ Prior ( $GL_1^2$ ) Model

The Gaussian  $L_1^2$  Norm Model ( $GL_1^2$ ) model is proposed by Brouwer & Lio (2017) based on the  $L_1^2$  norm for both  $\mathbf{W}, \mathbf{Z}$ .

**Prior** We assume  $\mathbf{W}$  and  $\mathbf{Z}$  are independently distributed with parameter  $\lambda_k^W$  and  $\lambda_k^Z$  proportional to a exponential function:

$$p(\mathbf{W}|\lambda_k^W) \propto \begin{cases} \exp \left[ -\frac{\lambda_k^W}{2} \sum_{m=1}^M \left( \sum_{k=1}^K w_{mk} \right)^2 \right], & \text{if } w_{mk} \geq 0 \text{ for all } m, k; \\ 0, & \text{if otherwise;} \end{cases} \quad (16)$$

$$p(\mathbf{Z}|\lambda_k^Z) \propto \begin{cases} \exp \left[ -\frac{\lambda_k^Z}{2} \sum_{n=1}^N \left( \sum_{k=1}^K z_{kn} \right)^2 \right], & \text{if } z_{kn} \geq 0 \text{ for all } n, k; \\ 0, & \text{if otherwise.} \end{cases}$$

Again, the prior for the noise variance  $\sigma^2$  is an inverse-gamma density with shape  $\alpha_\sigma$  and scale  $\beta_\sigma$ ,

$$p(\sigma^2) = \mathcal{G}^{-1}(\sigma^2 | \alpha_\sigma, \beta_\sigma) = \frac{\beta_\sigma^{\alpha_\sigma}}{\Gamma(\alpha_\sigma)} (\sigma^2)^{-\alpha_\sigma - 1} \exp\left(-\frac{\beta_\sigma}{\sigma^2}\right).$$

**Posterior** The conditional density of  $\sigma^2$  is the same as that in the GEE model (Eq. (15)). By Bayes' rule, the posterior is proportional to the product of likelihood and prior, it can be maximized to yield an estimate of  $\mathbf{W}$  and  $\mathbf{Z}$ :

$$\begin{aligned} & p(w_{mk} | \sigma^2, \mathbf{W}_{-mk}, \mathbf{Z}, \lambda_k^W, \mathcal{X}_k^Z, \mathbf{A}) = p(w_{mk} | \sigma^2, \mathbf{W}_{-mk}, \mathbf{Z}, \lambda_k^W, \mathbf{A}) \\ & \propto p(\mathbf{A} | \mathbf{W}, \mathbf{Z}, \sigma^2) \times p(\mathbf{W} | \lambda_k^W) = \prod_{i,j=1}^{M,N} \mathcal{N}(a_{ij} | \mathbf{w}_i^\top \mathbf{z}_j, \sigma^2) \times p(\mathbf{W} | \lambda_k^W) \\ & \propto \exp\left\{-\frac{1}{2\sigma^2} \sum_{i,j=1}^{M,N} (a_{ij} - \mathbf{w}_i^\top \mathbf{z}_j)^2\right\} \times \exp\left\{-\frac{\lambda_k^W}{2} \sum_{i=1}^M \left(\sum_{j=1}^K w_{ij}\right)^2\right\} \cdot u(w_{mk}) \\ & \propto \exp\left\{-\frac{1}{2\sigma^2} \sum_{j=1}^N (a_{mj} - \mathbf{w}_m^\top \mathbf{z}_j)^2\right\} \times \exp\left\{-\frac{\lambda_k^W}{2} \left(w_{mk} + \sum_{j \neq k} w_{mj}\right)^2\right\} \cdot u(w_{mk}) \\ & \propto \exp\left\{-\frac{1}{2\sigma^2} \sum_{j=1}^N \left(w_{mk}^2 z_{kj}^2 + 2w_{mk} z_{kj} \left(\sum_{i \neq k} w_{mi} z_{ij} - a_{mj}\right)\right)\right\} \exp\left\{-\frac{\lambda_k^W}{2} w_{mk}^2 - \lambda_k^W w_{mk} \sum_{j \neq k} w_{mj}\right\} u(w_{mk}) \\ & \propto \exp\left\{-\underbrace{\left(\frac{\sum_{j=1}^N z_{kj}^2 + \sigma^2 \lambda_k^W}{2\sigma^2}\right)}_{1/(2\widetilde{\sigma}_{mk}^2)} w_{mk}^2 + w_{mk} \underbrace{\left(-\lambda_k^W \cdot \sum_{j \neq k} w_{mj} + \frac{1}{\sigma^2} \sum_{j=1}^N z_{kj} \left(a_{mj} - \sum_{i \neq k} w_{mi} z_{ij}\right)\right)}_{\widetilde{\sigma}_{mk}^{-2} \widetilde{\mu}_{mk}}\right\} \cdot u(w_{mk}) \\ & \propto \mathcal{N}(w_{mk} | \widetilde{\mu}_{mk}, \widetilde{\sigma}_{mk}^2) \cdot u(w_{mk}) = \mathcal{TN}(w_{mk} | \widetilde{\mu}_{mk}, \widetilde{\sigma}_{mk}^2), \end{aligned} \tag{17}$$

where

$$\widetilde{\sigma}_{mk}^2 = \frac{\sigma^2}{\sum_{j=1}^N z_{kj}^2 + \sigma^2 \lambda_k^W}, \quad \widetilde{\mu}_{mk} = \left(-\lambda_k^W \cdot \sum_{j \neq k} w_{mj} + \frac{1}{\sigma^2} \sum_{j=1}^N z_{kj} \left(a_{mj} - \sum_{i \neq k} w_{mi} z_{ij}\right)\right) \cdot \widetilde{\sigma}_{mk}^2$$

are the posterior ‘‘parent’’ variance of the normal distribution, and the posterior ‘‘parent’’ mean of the normal distribution respectively. Note the posterior density of  $w_{mk}$  in Eq. (17) is very similar to that of the GEE model in Eq. (12) where we highlight the difference in red text.

**Connection to GEE** The second term  $\sigma^2 \lambda_k^W$  exists in the  $\text{GL}_1^2$  denominator of the variance  $\widetilde{\sigma}_{mk}^2$ . When all else are held equal, the  $\text{GL}_1^2$  has smaller variance than GEE, so the distribution of  $\text{GL}_1^2$  is more clustered in a smaller range. This is actually a stronger constraint/regularizer than GEE model.

### A.3. Gaussian Likelihood with $L_2^2$ Prior ( $\text{GL}_2^2$ ) Model

In the main paper, we further propose the  $\text{GL}_2^2$  model based on  $L_2$  norm.

**Prior** We assume  $\mathbf{W}$  and  $\mathbf{Z}$  are independently distributed with parameter  $\lambda_k^W$  and  $\lambda_k^Z$  proportional to a exponential function:

$$\begin{aligned}
 p(\mathbf{W}|\lambda_k^W) &\propto \begin{cases} \exp\left[-\frac{\lambda_k^W}{2} \sum_{m=1}^M \left(\sum_{k=1}^K w_{mk}^2\right)\right], & \text{if } w_{mk} \geq 0 \text{ for all } m, k; \\ 0, & \text{if otherwise;} \end{cases} \\
 p(\mathbf{Z}|\lambda_k^Z) &\propto \begin{cases} \exp\left[-\frac{\lambda_k^Z}{2} \sum_{n=1}^N \left(\sum_{k=1}^K z_{kn}^2\right)\right], & \text{if } z_{kn} \geq 0 \text{ for all } n, k; \\ 0, & \text{if otherwise.} \end{cases}
 \end{aligned} \tag{18}$$

Again, the prior for the noise variance  $\sigma^2$  is an inverse-gamma density with shape  $\alpha_\sigma$  and scale  $\beta_\sigma$ ,

$$p(\sigma^2) = \mathcal{G}^{-1}(\sigma^2|\alpha_\sigma, \beta_\sigma) = \frac{\beta_\sigma^{\alpha_\sigma}}{\Gamma(\alpha_\sigma)} (\sigma^2)^{-\alpha_\sigma-1} \exp\left(-\frac{\beta_\sigma}{\sigma^2}\right).$$

**Posterior** The conditional density of  $\sigma^2$  is the same as that in the GEE model (Eq. (15)). By Bayes' rule, the posterior is proportional to the product of likelihood and prior, it can be maximized to yield an estimate of  $\mathbf{W}$  and  $\mathbf{Z}$ :

$$\begin{aligned}
 &p(w_{mk}|\sigma^2, \mathbf{W}_{-mk}, \mathbf{Z}, \lambda_k^W, \lambda_k^Z, \mathbf{A}) = p(w_{mk}|\sigma^2, \mathbf{W}_{-mk}, \mathbf{Z}, \lambda_k^W, \mathbf{A}) \\
 &\propto p(\mathbf{A}|\mathbf{W}, \mathbf{Z}, \sigma^2) \times p(\mathbf{W}|\lambda_k^W) = \prod_{i,j=1}^{M,N} \mathcal{N}(a_{ij}|\mathbf{w}_i^\top \mathbf{z}_j, \sigma^2) \times p(\mathbf{W}|\lambda_k^W) \cdot u(w_{mk}) \\
 &\propto \exp\left\{-\frac{1}{2\sigma^2} \sum_{i,j=1}^{M,N} (a_{ij} - \mathbf{w}_i^\top \mathbf{z}_j)^2\right\} \times \exp\left\{-\frac{\lambda_k^W}{2} \sum_{i=1}^M \left(\sum_{j=1}^K w_{ij}^2\right)\right\} \cdot u(w_{mk}) \\
 &\propto \exp\left\{-\frac{1}{2\sigma^2} \sum_{j=1}^N (a_{mj} - \mathbf{w}_m^\top \mathbf{z}_j)^2\right\} \times \exp\left\{-\frac{\lambda_k^W}{2} w_{mk}^2\right\} \cdot u(w_{mk}) \\
 &\propto \exp\left\{-\frac{1}{2\sigma^2} \sum_{j=1}^N \left(w_{mk}^2 z_{kj}^2 + 2w_{mk} z_{kj} \left(\sum_{i \neq k}^K w_{mi} z_{ij} - a_{mj}\right)\right)\right\} \cdot \exp\left\{-\frac{\lambda_k^W}{2} w_{mk}^2\right\} \cdot u(w_{mk}) \\
 &\propto \exp\left\{-\underbrace{\left(\frac{\sum_{j=1}^N z_{kj}^2 + \sigma^2 \lambda_k^W}{2\sigma^2}\right)}_{1/(2\widetilde{\sigma}_{mk}^2)} w_{mk}^2 + w_{mk} \underbrace{\left(\frac{1}{\sigma^2} \sum_{j=1}^N z_{kj} \left(a_{mj} - \sum_{i \neq k}^K w_{mi} z_{ij}\right)\right)}_{\widetilde{\sigma}_{mk}^2 - 1 \quad \widetilde{\mu}_{mk}}\right\} \cdot u(w_{mk}) \\
 &\propto \mathcal{N}(w_{mk}|\widetilde{\mu}_{mk}, \widetilde{\sigma}_{mk}^2) \cdot u(w_{mk}) = \mathcal{TN}(w_{mk}|\widetilde{\mu}_{mk}, \widetilde{\sigma}_{mk}^2),
 \end{aligned} \tag{19}$$

where

$$\widetilde{\sigma}_{mk}^2 = \frac{\sigma^2}{\sum_{j=1}^N z_{kj}^2 + \sigma^2 \lambda_k^W}, \quad \widetilde{\mu}_{mk} = \left(\frac{1}{\sigma^2} \sum_{j=1}^N z_{kj} \left(a_{mj} - \sum_{i \neq k}^K w_{mi} z_{ij}\right)\right) \cdot \widetilde{\sigma}_{mk}^2$$

are the posterior ‘‘parent’’ variance of the normal distribution, and the posterior ‘‘parent’’ mean of the normal distribution respectively.

**Connection to GEE** We observe that the ‘‘parent’’ mean in the  $\text{GL}_2^2$  model is larger than that in the GEE model (Eq. (14)) since it does not contain the negative term  $-\lambda_{mk}^W$  in Eq. (14). While the variance is smaller than that in the GEE model (Eq. (13)) such that the conditional density of  $\text{GL}_2^2$  model is more clustered and it imposes a larger regularization.

#### A.4. Gaussian Likelihood with $L_\infty$ Prior (GL $_\infty$ ) Model

**Prior** We assume  $\mathbf{W}$  and  $\mathbf{Z}$  are independently distributed with parameter  $\lambda_k^W$  and  $\lambda_k^Z$  proportional to a exponential function:

$$p(\mathbf{W}|\lambda_k^W) \propto \begin{cases} \exp\left[-\lambda_k^W \sum_{m=1}^M \max_k |w_{mk}|\right], & \text{if } w_{mk} \geq 0 \text{ for all } m, k; \\ 0, & \text{if otherwise;} \end{cases} \quad (20)$$

$$p(\mathbf{Z}|\lambda_k^Z) \propto \begin{cases} \exp\left[-\lambda_k^Z \sum_{n=1}^N \max_k |z_{kn}|\right], & \text{if } z_{kn} \geq 0 \text{ for all } n, k; \\ 0, & \text{if otherwise.} \end{cases}$$

Note we remove the 2 in the denominator of  $\lambda_k^W$  for consistency issue which we will see shortly in the form of the conditional density in Eq. (21). Again, the prior for the noise variance  $\sigma^2$  is an inverse-gamma density with shape  $\alpha_\sigma$  and scale  $\beta_\sigma$ ,

$$p(\sigma^2) = \mathcal{G}^{-1}(\sigma^2|\alpha_\sigma, \beta_\sigma) = \frac{\beta_\sigma^{\alpha_\sigma}}{\Gamma(\alpha_\sigma)} (\sigma^2)^{-\alpha_\sigma-1} \exp\left(-\frac{\beta_\sigma}{\sigma^2}\right).$$

**Posterior** The conditional density of  $\sigma^2$  is the same as that in the GEE model (Eq. (15)). Denote  $\mathbf{1}(w_{mk})$  as the indicator whether  $w_{mk}$  is the largest one among  $k = 1, 2, \dots, K$ , the conditional density can be obtained by

$$\begin{aligned} p(w_{mk}|\sigma^2, \mathbf{W}_{-mk}, \mathbf{Z}, \lambda_k^W, \lambda_k^Z, \mathbf{A}) &= p(w_{mk}|\sigma^2, \mathbf{W}_{-mk}, \mathbf{Z}, \lambda_k^W, \mathbf{A}) \\ &\propto p(\mathbf{A}|\mathbf{W}, \mathbf{Z}, \sigma^2) \times p(\mathbf{W}|\lambda_k^W) = \prod_{i,j=1}^{M,N} \mathcal{N}(a_{ij}|\mathbf{w}_i^\top \mathbf{z}_j, \sigma^2) \times p(\mathbf{W}|\lambda_k^W) \cdot u(w_{mk}) \\ &\propto \exp\left\{-\frac{1}{2\sigma^2} \sum_{i,j=1}^{M,N} (a_{ij} - \mathbf{w}_i^\top \mathbf{z}_j)^2\right\} \times \exp\left\{-\lambda_k^W \cdot \sum_{i=1}^M \max_k |w_{ij}|\right\} \cdot u(w_{mk}) \\ &\propto \exp\left\{-\frac{1}{2\sigma^2} \sum_{j=1}^N (a_{mj} - \mathbf{w}_m^\top \mathbf{z}_j)^2\right\} \times \exp\{-\lambda_k^W \cdot w_{mk}\} \cdot u(w_{mk}) \cdot \mathbf{1}(w_{mk}) \\ &\propto \exp\left\{-\frac{1}{2\sigma^2} \sum_{j=1}^N \left(w_{mk}^2 z_{kj}^2 + 2w_{mk} z_{kj} \left(\sum_{i \neq k}^K w_{mi} z_{ij} - a_{mj}\right)\right)\right\} \cdot \exp\{-w_{mk} \cdot \lambda_k^W \cdot \mathbf{1}(w_{mk})\} \cdot u(w_{mk}) \\ &\propto \exp\left\{-\underbrace{\left(\frac{\sum_{j=1}^N z_{kj}^2}{2\sigma^2}\right)}_{1/(2\widetilde{\sigma}_{mk}^2)} w_{mk}^2 + w_{mk} \underbrace{\left(-\lambda_k^W \cdot \mathbf{1}(w_{mk}) + \frac{1}{\sigma^2} \sum_{j=1}^N z_{kj} \left(a_{mj} - \sum_{i \neq k}^K w_{mi} z_{ij}\right)\right)}_{\widetilde{\sigma}_{mk}^2 - 1 \widetilde{\mu}_{mk}}\right\} \cdot u(w_{mk}) \\ &\propto \mathcal{N}(w_{mk}|\widetilde{\mu}_{mk}, \widetilde{\sigma}_{mk}^2) \cdot u(w_{mk}) = \mathcal{TN}(w_{mk}|\widetilde{\mu}_{mk}, \widetilde{\sigma}_{mk}^2), \end{aligned} \quad (21)$$

where

$$\widetilde{\sigma}_{mk}^2 = \frac{\sigma^2}{\sum_{j=1}^N z_{kj}^2}, \quad \widetilde{\mu}_{mk} = \left(-\lambda_k^W \cdot \mathbf{1}(w_{mk}) + \frac{1}{\sigma^2} \sum_{j=1}^N z_{kj} \left(a_{mj} - \sum_{i \neq k}^K w_{mi} z_{ij}\right)\right) \cdot \widetilde{\sigma}_{mk}^2$$

are the posterior ‘‘parent’’ variance of the normal distribution, and the posterior ‘‘parent’’ mean of the normal distribution respectively.

**Connection to GEE** We observe that the ‘‘parent’’ variance in the GL $_\infty$  model is exactly the same as that in the GEE model (Eq. (13)). And when  $\mathbf{1}(w_{mk})$  is satisfied, the ‘‘parent’’ mean is the same as that in the GEE model as well (Eq. (14)). However, when  $w_{mk}$  is not the maximum value among  $\{w_{m1}, w_{m2}, \dots, w_{mK}\}$ , the ‘‘parent’’ mean is larger than that in the GEE model since the GL $_\infty$  model excludes this negative term. The GL $_\infty$  model then has the interpretation that it has a *sparsity constraint* when  $w_{mk}$  is the maximum value; and it has a *relatively loose constraint* when  $w_{mk}$  is not the maximum value. Overall, the GL $_\infty$  favors a loose regularization compared with the GEE model.